PHYSICAL REVIEW B **82**, 205118 (2010)

Metal-insulator transitions in TiO_2/VO_2 superlattices

Keisuke Shibuya,[1,*] Masashi Kawasaki,[1,2] and Yoshinori Tokura[1,3,4]
[1]*Cross-correlated Materials Research Group (CMRG) and Correlated Electron Research Group (CERG), Advanced Science Institute, RIKEN, Wako 351-0198, Japan*
[2]*WPI Advanced Institute for Materials Research, Tohoku University, Sendai 980-8577, Japan*
[3]*Department of Applied Physics, University of Tokyo, Tokyo 113-8656, Japan*
[4]*Multiferroics Project, ERATO, Japan Science and Technology Agency (JST), Tokyo 113-8656, Japan*
(Received 8 September 2010; published 19 November 2010)

We have fabricated a series of superlattices composed of $V_{1-x}W_xO_2$ ($x=0$ or 0.08 with $1+2x$ d electron per V atom) and TiO_2 (no d electron) to investigate the interface and carrier-confinement effects of the metal-insulator phenomena of VO_2. This study was also motivated by the prediction of a half-metallic state with a semi-Dirac point at the TiO_2/VO_2 interface [V. Pardo and W. E. Pickett, Phys. Rev. Lett. **102**, 166803 (2009)]. The growth conditions of the superlattices were optimized so that we could reproduce the known electronic states for the constituent compounds in case of the single-layer films, namely, VO_2 exhibiting a paramagnetic metal to spin-singlet insulator transition at around room temperature, $V_{0.92}W_{0.08}O_2$ ($W:VO_2$) being metallic down to the lowest temperature, and TiO_2 being a wide-gap band insulator. We found no metallic ground state in these superlattices in contradiction with the theoretical prediction. The TiO_2/VO_2 superlattices always show a resistive transition, corresponding to the metal-insulator transition in the VO_2 single layer, at around 300 K for the VO_2-layer thickness varying from 15 monolayers (ML) down to 3 ML. The resistive transition is accompanied with the structural change, consistent with the V-V dimerization in VO_2 along c axis, suggesting the robust spin-singlet bond formation as well as the dimeric lattice distortion persistent even at the TiO_2/VO_2 interface. In the case of $TiO_2/W:VO_2$ superlattices, the insulating ground state revives while the metal-insulator transition temperature decreases from 230 to 95 K as the $W:VO_2$ thickness is increased from 10 to 40 ML. These results indicate the persistent competition between the spin-singlet bond formation and the kinetic energy of correlated electrons regulated by the $W:VO_2$ thickness.

DOI: 10.1103/PhysRevB.82.205118 PACS number(s): 73.20.−r, 73.21.Cd, 73.40.−c

I. INTRODUCTION

VO_2 shows a $3d^1$ electron configuration and undergoes a metal-insulator transition at around 340 K, accompanied by a structural change from a high-temperature rutile (tetragonal) to a low-temperature monoclinic form.[1] Dimerization of V ions occurs in the latter with a tiling of the V-V bond from c axis. It makes $3d$ electrons localized on V sites forming spin singlet.[2] The magnetic susceptibility changes from paramagnetic to nonmagnetic upon the transition. VO_2 has recently been of particular interest for possible device application due to the fact that the transition occurs above room temperature with a huge jump in resistivity. Field-effect devices[3] and photoinduced switches[4] have been demonstrated with using VO_2 as the active layers. The metal-insulator phenomena in VO_2 can be controlled by electron doping in epitaxial $V_{1-x}W_xO_2$ thin films which can reach a metallic ground state at around $x=0.08$ ($W:VO_2$).[5]

Recently, Pardo and Pickett suggested by the density-functional theory that a half-metallic VO_2 slab can be realized by confining VO_2 with insulating TiO_2 layers, where a semi-Dirac-point Fermi surface emerges in $(TiO_2)_m/(VO_2)_n$ superlattices at $m=5$ and $n=3$.[6] TiO_2 is a band insulator with $3d^0$ configuration and has a band gap of about 3.0 eV. As a consequence of quantum confinement of the d electrons in the VO_2 layers along c axis, a collective structural dimerization along the c axis is predicted to be suppressed and thereby the VO_2 layer to remain in the metallic state. The metal-insulator transition is predicted to occur through a semi-Dirac-point phase between $n=3$ and 4, which will not be accompanied by any structural changes. The band-dispersion crossing occurs at a single point in momentum (k) space and the electrons behave as massless along the zone diagonal direction in k space and massive along the perpendicular direction. Such a semi-Dirac point is not destroyed with spin-orbital coupling. A single VO_2/TiO_2 interface has been previously investigated and no metallic state was observed.[7] However, superlattice structures have not yet been constructed so far. In order to examine the theoretical prediction, the layer thicknesses of VO_2 and TiO_2 have to be controlled in an atomic scale.

While partly motivated by the theoretical prediction on the exotic half-metallic state, we have also intended to explore possible novel phenomena of the TiO_2/VO_2 superlattice systems related to the metal-insulator transitions coupled with the lattice-structural transition. The superlattices have seldom been examined for binary-oxide rutile structures whereas high-quality interfaces and superlattice structures have been well developed in ternary perovskite-type oxides.[8] Examples of d^1/d^0 superlattices are $LaTiO_3/SrTiO_3$ and $SrVO_3/SrTiO_3$. When a Mott insulator $LaTiO_3$ is sandwiched by a band-insulator $SrTiO_3$ with chemically abrupt interfaces, the film shows a metallic behavior, indicating charge penetration from $LaTiO_3$ to $SrTiO_3$.[9] The conducting interfaces between the two insulators were confirmed by photoemission study[10] and optical spectroscopy.[11] The exotic metallic behavior at this interface has also been theoretically studied.[12] As another example, when metallic $SrVO_3$ is con-

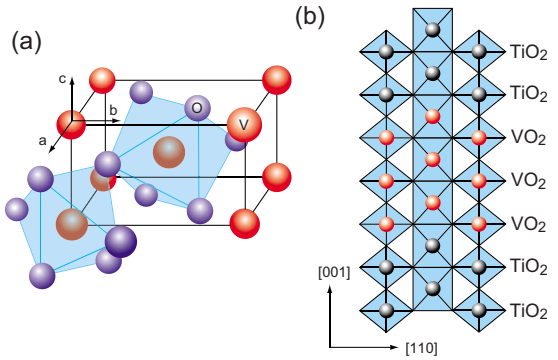

FIG. 1. (Color online) Schematic view of (a) VO_2 structure and (b) (001)-oriented $TiO_2/VO_2/TiO_2$ structure, where the thickness of the VO_2 layer is 3 ML.

fined with $SrTiO_3$, a metal-insulator transition takes place depending on the $SrVO_3$ thickness.[13,14] At a single $SrVO_3/SrTiO_3$ interface, a pseudogap starts to be formed at Fermi energy with decreasing $SrVO_3$ layer thickness, which is interpreted in terms of the crossover from three to two dimensions.[15]

One of the differences of rutile superlattices from those of perovskite is the cation-cation distance. In both cases, transition-metal ions form octahedra with oxygen ions. In perovskite, the cation-cation distance along c axis is about 0.39 nm due to corner sharing of octahedra whereas those in rutile are about 0.29 nm as depicted in Fig. 1(a) due to edge sharing. Moreover, the edge-sharing octahedra forms one-dimensional chain along c axis and the overlap of wave function within ab plain is expected to be much smaller than that of perovskite. Therefore, the interface effects of rutile will be even more significant than those of perovskite due to the difference in the balance of electron-correlation energy and kinetic energy of electrons. Figure 1(b) displays three unit cells of VO_2 between TiO_2 slabs. The collective V-V dimerization in VO_2 is expected to be suppressed by the insertion of TiO_2 layers in the (001)-oriented superlattices.

In this work, we constructed $TiO_2/V_{1-x}W_xO_2$ (x=0 or 0.08) superlattices on TiO_2 (001) substrates. The effect of quantum confinement was examined in nondoped and electron-doped VO_2 layers with TiO_2 layers as the intervening barrier. For the both superlattices, the metal-insulator transition is so robust that no metallic ground state is realized. However, different features were found between the TiO_2/VO_2 and $TiO_2/W:VO_2$ superlattices, in particular, in the VO_2 or $W:VO_2$ thickness dependence on the metal-insulator transition temperature (T_{MI}). The results are argued comprehensively in terms of the robust spin-singlet formation causing the lattice dimerization that competes with the kinetic energy of correlated electrons in the VO_2 (or $W:VO_2$) layer.

II. TiO_2/VO_2 SUPERLATTICES

A. Growth optimization of individual films

Although the growth conditions of individual compounds have been well established, we have to fabricate both constituent layers with desired physical properties under the same condition which can be applied for the fabrication of superlattices. We first explored such a growth condition; the TiO_2 and VO_2 thin films were grown, respectively, on (001) surfaces of TiO_2 single-crystal substrates (purchased from Shinkosha Co., Ltd.) by a pulsed laser deposition method. The substrate temperature and the oxygen pressure were kept at 350 °C and at 3–10 mTorr, respectively, during the deposition. Substrate temperature above 400 °C resulted in a considerable interdiffusion of V and Ti ions across the interfaces, which has to be minimized to construct a chemically sharp interface. Details of the fabrication procedure for VO_2 epitaxial film on TiO_2 substrate were described elsewhere.[5] Resistivity was measured with a conventional four-probe method employing Au/Ti double-layer electrodes deposited by electron-beam evaporation through a stencil mask. Transport properties were examined with physical property measurement system (PPMS; Quantum Design) and magnetic properties were investigated with magnetic property measurement system (MPMS; Quantum Design). X-ray diffraction (XRD) was measured at room temperature unless mentioned specifically.

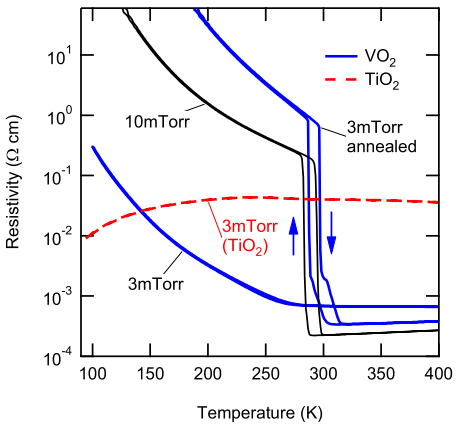

FIG. 2. (Color online) Electrical resistivity of VO_2 (solid lines) and TiO_2 (a dashed line) single (non-superlattice)-layer films grown on TiO_2 (001) substrates at different oxygen pressures. The growth temperature was kept at 350 °C. The conductivity of TiO_2 films can be eliminated with annealing at 350 °C in an oxygen pressure of 1 Torr for 1 h (not shown). The annealing can compensate oxygen vacancies in VO_2 as well as in TiO_2 layers. The annealed VO_2 film grown at an oxygen pressure of 3 mTorr shows a clear resistivity jump at T_{MI}, which is comparable to that grown at a high oxygen pressure of 10 mTorr. The film thickness of VO_2 is about 10 nm.

We found that TiO_2 films have to be grown well below 10 mTorr especially at such a low substrate temperature in order to realize a flat surface and a high crystallinity. The TiO_2 film deposited at an oxygen pressure of 10 mTorr was amorphous. Temperature dependence of resistivity for a TiO_2 homoepitaxial film grown at 3 mTorr is shown in Fig. 2. Due to oxygen vacancies generated during the growth under such a low oxygen pressure, the TiO_2 film showed a metallic conductivity. Annealing procedure at 350 °C in an oxygen pressure of 1 Torr for 1 h after the deposition was found to eliminate the conductivity by compensating oxygen vacancies in the film (not shown).

Figure 2 also depicts resistivity data for a 10-nm-thick VO_2 film fabricated on TiO_2 (001) under various oxygen pressures. The film grown at an oxygen pressure of 10 mTorr exhibited a well-defined metal-insulator transition with a hysteresis as desired. However, this condition is not compatible with that for growing insulating TiO_2 film. When oxygen pressure was reduced to 3 mTorr, the metal-insulator transition was almost suppressed due to oxygen vacancies, which is consistent with a previous report.[16] The annealing employed for the TiO_2 film was also effective for the VO_2 film to recover the desired metal-insulator transition as shown in Fig. 2.

B. Structure and properties of TiO_2/VO_2 superlattices

According to the optimized recipe described in the previous section, all the TiO_2/VO_2 superlattices were fabricated on TiO_2 (001) substrates; namely, at a substrate temperature of 350 °C and an oxygen pressure of 3 mTorr followed by an annealing procedure under an oxygen pressure of 1 Torr for 1 h. In this growth condition, both TiO_2 and VO_2 layers show their expected properties. The layer thicknesses of constituent layers in superlattices were regulated by the deposition duration. The thickness of TiO_2 was maintained at 5 monolayers (ML) so as to mimic the theoretically predicted situation.[6] The total thickness of the superlattices was set at around 60 nm. The XRD patterns for a series of $(TiO_2)_5/(VO_2)_n$ superlattices are shown in Fig. 3(a). The peaks assignable to 002 reflections (arrows) are clearly seen, thereby confirming the (001)-oriented epitaxial growth of TiO_2/VO_2 superlattices. The average lattice constant of the superlattices systematically decreases with increasing thickness of the VO_2 layer. The c-axis lattice constants of TiO_2, VO_2 (rutile), and VO_2 (monoclinic) thin films pseudomorphically grown on TiO_2 (001) are 0.296 nm, 0.283 nm, and 0.285 nm, respectively. X-ray reciprocal space mapping data indicates that the $(TiO_2)_5/(VO_2)_n$ superlattices have a pseudomorphic structure with identical in-place lattice constant (a=0.459 nm). Tiny lattice-relaxation behavior starts to be observed with increasing n above 5, e.g., in the [5/15] superlattice. Figure 3(b) shows the temperature dependence of the average lattice constant of the [5/10] and [5/15] superlattices above room temperature. The lattice constants decrease with increasing temperature around 300–320 K due to the structural change in VO_2 from low-temperature monoclinic to high-temperature rutile. The inset shows XRD patterns around 002 diffraction peak of the [5/10] superlattice at various temperatures from 300 to 321 K. These results denote that the majority of the VO_2 layer in the superlattices is monoclinic at room temperature (300 K) although the phase transition seems to be completed at lower temperatures and not yet at 300 K. The structure difference and coexistence of TiO_2 (rutile) and VO_2 (monoclinic) resulted in the degraded XRD patterns in Fig. 3(a). In fact, the sharp XRD patterns with well-defined Laue fringes were observed for $TiO_2/W:VO_2$ superlattices with both rutile structures at room temperature (see Sec. III B and Fig. 5).

Figure 4 presents temperature dependence of resistivity for the TiO_2/VO_2 superlattices with varying VO_2 layer

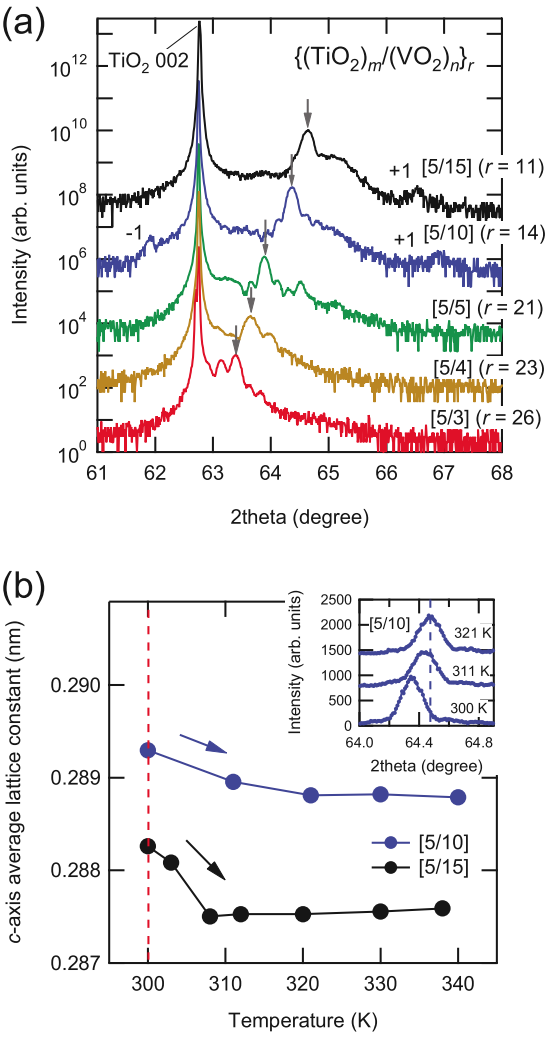

FIG. 3. (Color online) (a) XRD patterns of the $(TiO_2)_5/(VO_2)_n$ (n=3, 4, 5, 10, and 15) superlattices around TiO_2 002 diffraction peak. The arrows indicate principal diffractions of superlattices that reflect the average lattice constant. The satellite peaks reflecting the periodicity is denoted by +1 and −1. The designed periodicity is denoted by $[m/n]$ and the repetition is denoted by r. (b) Temperature dependence of the c-axis average lattice constants of the [5/10] and [5/15] superlattices. The lattice shrinks around 300–320 K with increasing temperature from room temperature, corresponding to a structural transition of VO_2. The inset shows XRD patterns around 002 diffraction peak of the [5/10] superlattice at various temperatures.

thickness. All the superlattices show thermal hystereses in resistivity at around 310 K, indicating a structural transition of VO_2 layers. This is consistent with the result of the structural characterization. Hereafter, we refer this structural transition temperature as T_{MI}, even though not fully metallic above T_{MI} in these superlattices. With increasing the VO_2-layer thickness to 10 ML, the resistivity decreases and its jump at T_{MI} becomes sharper; namely, the thermal behavior approaches to that of a single-layer VO_2 film. The [5/15] film exhibits a broader transition, suggesting an effect of microcracks which have been previously reported in VO_2 films.[17] There, a number of lines representing cracks were observed in atomic force microscope images above the criti-

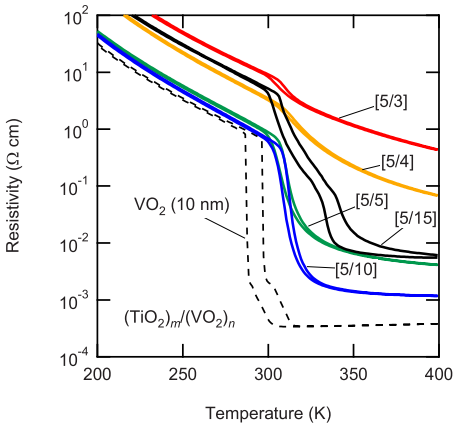

FIG. 4. (Color online) Temperature dependence of resistivity for the $(TiO_2)_5/(VO_2)_n$ superlattices. The data (a broken line) of a single-layer VO_2 film are also depicted for comparison. Resistivity change at the transition becomes more pronounced with increasing the VO_2 layer thickness.

cal thickness of 15 nm (50 ML). For these superlattices, no metallic ground states were observed at low temperatures, although predicted theoretically for $n \geq 3$.[6] Furthermore, no ferromagnetic signal was detected. The apparent difference from the theoretical prediction is the extremely robust V-V dimerization which can survive in reality even when the VO_2 layer is as thin as 3 ML. No appreciable shift of T_{MI} indicates that the VO_2 characteristics are not affected by the insertion of TiO_2 slabs. Even the [5/3] superlattice shows a small resistivity jump with a thermal hysteresis at T_{MI}, indicating a persistent structural change; this is again in contrast to the theoretical prediction that the metal-insulator transition will not occur with any structural changes.

III. $TiO_2/W:VO_2$ SUPERLATTICES

Since the metallic ground state was not observed for the TiO_2/VO_2 superlattices, the inherently metallic $W:VO_2$ layer was alternatively utilized as the component layer for the superlattice. It has recently been clarified for the single-layer $V_{1-x}W_xO_2$ that V-V dimerization is systematically destabilized with W doping and that the T_{MI} is monotonically reduced with W concentration (x) up to 8% substitution.[5] We chose the composition of $V_{0.92}W_{0.08}O_2$ ($x=0.08$) that shows a metallic behavior in a whole temperature region below 400 K in case of the single-layer film.

A. Growth optimization of individual films

The crystallinity of $W:VO_2$ films grown at an oxygen pressure of 3 mTorr was as good as that of the films grown under a higher pressure of 20 mTorr. However, the low-pressure-grown films show distinct metal-insulator transition at around 100 K (not shown) while the films grown at an oxygen pressure of 20 mTorr exhibit a metallic ground state.[5] This is perhaps because the W ion as the donor is not fully oxidized in such a low pressure. Therefore, we employed an ozone (O_3) atmosphere (introduced directly from an ozonizer) for growing $W:VO_2$ films with keeping the substrate

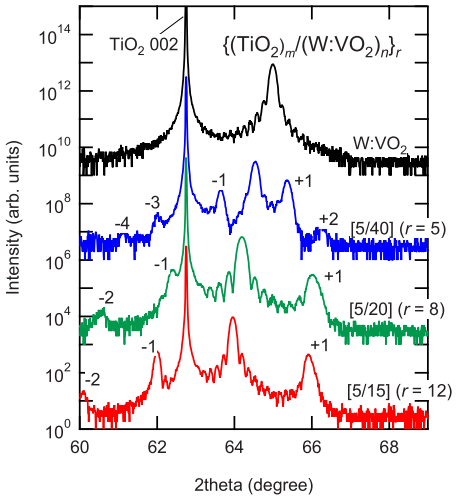

FIG. 5. (Color online) XRD patterns of the $V_{0.92}W_{0.08}O_2$ ($W:VO_2$) single-layer film and the $(TiO_2)_5/(W:VO_2)_n$ ($n=15$, 20, and 40) superlattices around TiO_2 002 diffraction peak. The designed periodicity is denoted by $[m/n]$ and the repetition is denoted by r. Clear Laue fringes and superlattice satellite peaks are seen because both TiO_2 and $W:VO_2$ have rutile (tetragonal) structure at room temperature and show the atomically sharp interfaces.

temperature at 350 °C. The $W:VO_2$ film grown at 3 mTorr of O_2/O_3 showed a comparable crystallinity with that deposited at 20 mTorr oxygen pressure. The O_2/O_3 environment is thus turned out not to be harmful to the epitaxial growth of TiO_2 films. Therefore, $TiO_2/W:VO_2$ superlattices were fabricated on TiO_2 (001) substrates at a temperature of 350 °C and O_2/O_3 pressure of 3 mTorr followed by an annealing procedure under an oxygen pressure of 1 Torr for 1 h. The total film thickness was set at 60–70 nm and the thickness of TiO_2 was kept at 5 ML as in the case of the TiO_2/VO_2 superlattices so as to facilitate the straightforward comparison of the both cases.

B. Structure and properties of $TiO_2/W:VO_2$ superlattices

Figure 5 shows the XRD patterns of a single-layer $W:VO_2$ ($V_{0.92}W_{0.08}O_2$) film and $(TiO_2)_5/(W:VO_2)_n$ ($n=15$, 20, and 40) superlattices. The single-layer film was fabricated under the optimized condition as described in the previous section. The c-axis lattice constant of $V_{0.92}W_{0.08}O_2$ is 0.287 nm. Clear Laue fringes and superlattice satellite peaks are seen, indicating both TiO_2 and $W:VO_2$ are high-temperature rutile (tetragonal) phases at room temperature in contrast to TiO_2/VO_2 superlattices. From these diffraction peaks, the film thickness was deduced to be 60–70 nm and the structures of superlattices were confirmed to be as designed. Pseudomorphic growth was confirmed for the all superlattices without lattice relaxation. The sharp interfaces within the superlattice were also confirmed (not shown in figures) by the secondary ion mass spectroscopy, although its resolution was limited to 2–3 nm.

Temperature dependence of resistivity for the $(TiO_2)_5/(W:VO_2)_n$ superlattices is presented in Fig. 6. Although the resistivity is decreased as the $W:VO_2$ layer thick-

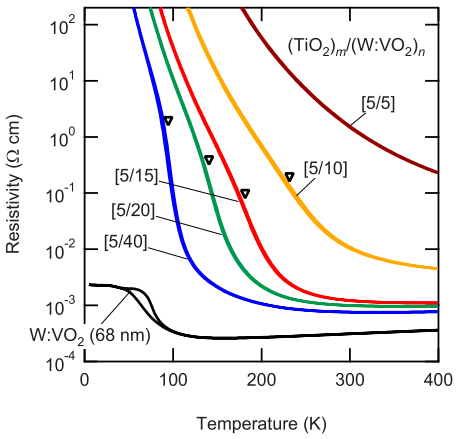

FIG. 6. (Color online) Temperature dependence of resistivity for the $(TiO_2)_5/(W:VO_2)_n$ superlattices. The data for a single-layer $W:VO_2$ film are also presented for comparison. All the superlattices show metal-insulator transitions at various temperatures in contrast to the metallic ground state of the single-layer film, indicating less itinerant characteristics due to confinement. The metal-insulator transition temperature, T_{MI}, (open triangles) is determined as the inflection point of the temperature-resistivity curve.

ness is increased from $n=5$ to 40, the metal-insulator transition is persistently observed and the resistivity in a metallic temperature region is considerably higher than that of the single-layer $W:VO_2$ film. These results imply that the carrier dynamics in the $W:VO_2$ layer suffers from scattering at the interfaces as well as reduction in the bandwidth due to the two-dimensional confinement. Recently, Yoshimatsu *et al.* found a dimensional-crossover-driven metal-insulator transition in $SrVO_3$ on $SrTiO_3$ surface, a heterostructure composed of $3d^1/3d^0$ system.[15] They found that at least 3 ML (1.2 nm) of $SrVO_3$ is necessary for a finite density of states at Fermi energy. The observed transition to the insulating ground state is ascribed to the reduction in the bandwidth. A similar scenario appears applicable to the present case, although the critical thickness seems to be much larger in the $W:VO_2/TiO_2$ system. The difference may be understood by considering that VO_2 with rutile structure has a larger bandwidth along c axis than in the ab plane and hence is more amenable to the electronic confinement along the c axis in the superlattices.

IV. PHASE DIAGRAM

Figure 7(a) presents the variation in T_{MI} with the thickness of VO_2 or $W:VO_2$ layers in the both series of superlattices. The transition temperature, T_{MI}, is defined from resistivity (ρ) data as the inflection points in $d[\ln(\rho)]/d(1/T)$ versus temperature (T) plots. There can be seen no shift in T_{MI} for the TiO_2/VO_2 superlattices as mentioned above. The V-V dimerization in VO_2 is so robust against the confinement when the filling is kept as d^1 as in the present case. On the contrary, the T_{MI} for the $TiO_2/W:VO_2$ superlattices increases with reducing the $W:VO_2$ layer thickness. One of the possible origins for the T_{MI} shift is the charge transfer from $W:VO_2$ layer to TiO_2 layer across the interface. To check

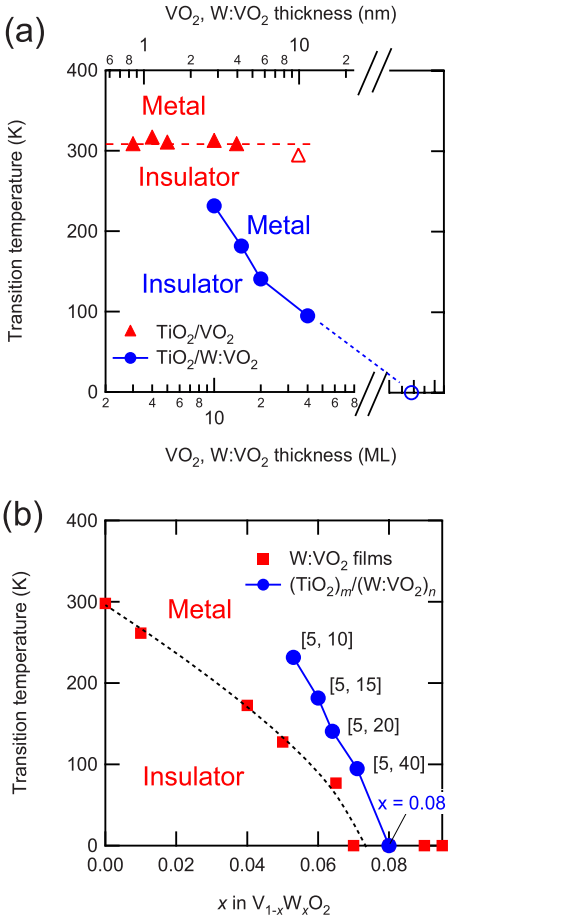

FIG. 7. (Color online) (a) The metal-insulator transition temperatures (T_{MI}) deduced from resistivity data are plotted as a function of layer thickness of VO_2 or $W:VO_2$. The layer thickness of TiO_2 is fixed at 5 ML. The T_{MI} of TiO_2/VO_2 superlattices (closed triangles) is nearly independent of VO_2 layer thickness whereas that of $TiO_2/W:VO_2$ (closed circles) critically increases as the $W:VO_2$ layer thickness is reduced. Those of single-layer VO_2 (open triangle) and $W:VO_2$ (open circle) are presented for comparison. Dashed lines are merely the guide to the eyes. (b) A metal-insulator phase diagram in $V_{1-x}W_xO_2$ ($0 \le x \le 0.095$) film (squares). The T_{MI} of the $(TiO_2)_5/(W:VO_2)_n$ superlattices (circles) is plotted, assuming the excess d electron in the $W:VO_2$ layer is uniformly distributed over the whole superlattice.

this possibility, we plot the T_{MI} of superlattices [Fig. 7(b)] on the x vs T_{MI} phase diagram of $V_{1-x}W_xO_2$ ($x<0.095$) system,[5] assuming the excess d electron (0.08×2 per V atom) is evenly distributed over the entire film. The deviation indicates that the T_{MI} shift cannot be solely explained by this simple scenario of charge transfer; electrons mainly localize in the constituent VO_2 layer due to the discontinuity of VO_2 conduction chain along c axis by the insertion of TiO_2 layers.

The VO_2 (or $W:VO_2$) layer thickness (m ML) dependence of the T_{MI} is quite different between the two cases of TiO_2/VO_2 and $TiO_2/W:VO_2$ superlattices. It is known that the lattice-structural transition of the VO_2 layers at T_{MI} is dominated by the local spin-singlet (valence-bond solid; VBS) formation originating from the strongly correlated t_{2g} electron with $S=1/2$.[18] The important implication from the

minimal m dependence of T_{MI} for the TiO_2/VO_2 superlattices is that such dimeric lattice distortion is of short range in nature, yet the lattice strain filed may survive across the interface. When the band filling of VO_2 is changed, by contrast, the metallic state tends to be stabilized even in the electron-confined superlattices. Nevertheless, the kinetic energy of the correlated electrons is still too small to realize the true metallic ground state for the investigated superlattices ($m \leq 40$) and the $W:VO_2$ layers are readily amenable to the lattice-dimeric spin-singlet formation at low temperatures; the excess carriers in the dimerized lattice below T_{MI} seem to be well localized perhaps due to the self-trapping process. Then, the competition between the electron kinetic energy controlled by the $W:VO_2$ thickness (m) and the spin-singlet (VBS) formation may produce the steep m dependence of T_{MI} as observed for the $TiO_2/W:VO_2$ superlattices. The contradiction to the theoretically predicted half-metallic state in the TiO_2/VO_2 superlattices is thus ascribable to the stronger electron correlation leading to the local spin-singlet formation irrespective of deviations from half band filling or even number of m (VO_2 layer thickness) as well as to the stronger electron-lattice interaction producing the lattice strain field of longer range than originally anticipated.

V. CONCLUSIONS

We have fabricated rutile-type superlattices of TiO_2/VO_2 and $TiO_2/W:VO_2$. The metal-insulator transition near room temperature was persistently observed in the TiO_2/VO_2 superlattices. Unlike the theoretical prediction by Pardo and Pickett,[6] the metal-insulator transition is accompanied with the structural change in VO_2 even when the layer is as thin as 3 ML. The quantum confinement of VO_2 layer with TiO_2 slabs does not suppress the collective V-V dimerization. The T_{MI} of the TiO_2/VO_2 superlattices is independent of the VO_2 layer thickness. A half-metallic behavior as proposed[6] was not observed. When we add electrons in VO_2 layers with employing $TiO_2/W:VO_2$ superlattices, the T_{MI} is reduced with the increase in the $W:VO_2$ layers thickness ($d_{W:VO_2}$) but the insulating phase cannot be diminished up to $d_{W:VO_2}=40$ ML, resulting in no metallic ground states. In this case, the steep $d_{W:VO_2}$ dependence of T_{MI} can be ascribed to the competition between the electron kinetic energy regulated by $d_{W:VO_2}$ and the spin-singlet formation. The observed robust lattice-structural transition in most of the superlattices thus arises from such a local electron-lattice interaction characteristic of this highly correlated electron ($S=1/2$) system as well as the possible long-range lattice strain field.

ACKNOWLEDGMENTS

The authors thank J. S. Lee and D. Okuyama for useful discussions. This work was supported by the Japan Society for the Promotion of Science (JSPS) through its Funding Program for World-Leading Innovative R&D on Science and Technology (FIRST Program) and by Grants-in-Aid for young scientists (B) (Grant No. 22760016).

*k.shibuya@riken.jp

[1] F. J. Morin, Phys. Rev. Lett. **3**, 34 (1959).
[2] J. B. Goodenough, J. Solid State Chem. **3**, 490 (1971).
[3] D. Ruzmetov, G. Gopalakrishnan, C. Ko, V. Narayanamurti, and S. Ramanathan, J. Appl. Phys. **107**, 114516 (2010).
[4] A. Cavalleri, Th. Dekorsy, H. H. W. Chong, J. C. Kieffer, and R. W. Schoenlein, Phys. Rev. B **70**, 161102(R) (2004).
[5] K. Shibuya, M. Kawasaki, and Y. Tokura, Appl. Phys. Lett. **96**, 022102 (2010).
[6] V. Pardo and W. E. Pickett, Phys. Rev. Lett. **102**, 166803 (2009); Phys. Rev. B **81**, 035111 (2010).
[7] K. Maekawa, M. Takizawa, H. Wadati, T. Yoshida, A. Fujimori, H. Kumigashira, M. Oshima, Y. Muraoka, Y. Nagao, and Z. Hiroi, Phys. Rev. B **76**, 115121 (2007).
[8] J. Mannhart and D. G. Schlom, Science **327**, 1607 (2010).
[9] A. Ohtomo and H. Y. Hwang, Nature (London) **427**, 423 (2004).
[10] M. Takizawa, H. Wadati, K. Tanaka, M. Hashimoto, T. Yoshida, A. Fujimori, A. Chikamatsu, H. Kumigashira, M. Oshima, K. Shibuya, T. Mihara, T. Ohnishi, M. Lippmaa, M. Kawasaki, H. Koinuma, S. Okamoto, and A. J. Millis, Phys. Rev. Lett. **97**, 057601 (2006).
[11] S. S. A. Seo, W. S. Choi, H. N. Lee, L. Yu, K. W. Kim, C. Bernhard, and T. W. Noh, Phys. Rev. Lett. **99**, 266801 (2007).
[12] S. Okamoto and A. J. Millis, Nature (London) **428**, 630 (2004).
[13] H. Koinuma, M. Yoshimoto, H. Nagata, and T. Tsukahara, Solid State Commun. **80**, 9 (1991).
[14] D. H. Kim, D.-W. Kim, B. S. Kang, T. W. Noh, D. R. Lee, K.-B. Lee, and S. J. Lee, Solid State Commun. **114**, 473 (2000).
[15] K. Yoshimatsu, T. Okabe, H. Kumigashira, S. Okamoto, S. Aizaki, A. Fujimori, and M. Oshima, Phys. Rev. Lett. **104**, 147601 (2010).
[16] K. Nagashima, T. Yanagida, H. Tanaka, and T. Kawai, J. Appl. Phys. **100**, 063714 (2006).
[17] K. Nagashima, T. Yanagida, H. Tanaka, and T. Kawai, Phys. Rev. B **74**, 172106 (2006).
[18] T. M. Rice, H. Launois, and J. P. Pouget, Phys. Rev. Lett. **73**, 3042 (1994).